JCTC Journal of Chemical Theory and Computation

Membrane/Toxin Interaction Energetics via Serial Multiscale Molecular Dynamics Simulations

Chze Ling Wee, Martin B. Ulmschneider,† and Mark S. P. Sansom*

Department of Biochemistry and Oxford Centre for Integrative Systems Biology, University of Oxford, South Parks Road, Oxford, OX1 3QU, United Kingdom

Received December 4, 2009

Abstract: Computing free energies of complex biomolecular systems via atomistic (AT) molecular dynamics (MD) simulations remains a challenge due to the need for adequate sampling and convergence. Recent coarse-grained (CG) methodology allows simulations of significantly larger systems ($\sim 10^6$ to 10^8 atoms) over longer (μs/ms) time scales. Such CG models appear to be capable of making semiquantitative predictions. However, their ability to reproduce accurate thermodynamic quantities remains uncertain. We have recently used CG MD simulations to compute the potential of mean force (PMF) or free energy profile of a small peptide toxin interacting with a lipid bilayer along a 1D reaction coordinate. The toxin studied was VSTx1 (Voltage Sensor Toxin 1) from spider venom which inhibits the archeabacterial voltage-gated potassium (Kv) channel KvAP by binding to the voltage-sensor (VS) domains. Here, we re-estimate this PMF profile using (i) AT MD simulations with explicit membrane and solvent and (ii) an implicit membrane and solvent (generalized Born; GBIM) model where only the peptide was explicit. We used the CG MD free energy simulations to guide the setup of the corresponding AT MD simulations. The aim was to avoid local minima in the AT simulations which would be difficult over shorter AT time scales. A cross-comparison of the PMF profiles revealed a conserved topology, although there were differences in the magnitude of the free energies. The CG and AT simulations predicted a membrane/water interface free energy well of −27 and −23 kcal/mol, respectively (with respect to water). The GBIM model, however, gave a reduced interfacial free energy well (−12 kcal/mol). In addition, the CG and GBIM models predicted a free energy barrier of +61 and +96 kcal/mol, respectively, for positioning the toxin at the center of the bilayer, which was considerably smaller in the AT simulations (+26 kcal/mol). Thus, we present a framework for serially combining CG and AT simulations to estimate the free energy of peptide/membrane interactions. Such approaches for combining simulations at different levels of granularity will become increasingly important in future studies of complex membrane/protein systems.

Introduction

Accurate determination of free energies is crucial for the understanding of various biophysical systems. Molecular dynamics (MD) simulations have been used to estimate free energies, e.g., by counting the number of events along the reaction coordinate(s) of interest.[1] In the context of membrane proteins and channels, for example, MD simulations have been used to calculate the free energy of ion conduction through ion channels[2,3] and related pores,[4,5] and the free energy of partitioning of amino acid side chain analogues into lipid bilayers.[6] These calculations are founded on the basis that well sampled distributions can be obtained from

* To whom correspondence should be addressed. Phone: +44 1865 613306. Fax: +44 1865 613238. E-mail: mark.sansom@bioch.ox.ac.uk.

† Current address: Department of Physiology and Biophysics, University of California at Irvine, Irvine, CA 92697-4560.

10.1021/ct900652s
Published on Web 02/04/2010

finite-time simulations. Atomistic (AT) MD simulations can routinely address systems of $\sim 10^5$ to 10^6 atoms over $\sim 10^2$ to 10^3 ns. This is likely to be insufficient for sampling all but the simplest systems.[1] For example, many biophysical processes of interest (e.g., ion channel gating) occur over longer (e.g., >1 μs) time scales. Thus, achieving adequate sampling in free energy simulations of membrane/protein systems remains challenging.

Recent coarse-grained (CG) simulation methodology has generated considerable interest as it permits simulations of larger systems over longer time scales.[7−15] In the context of membrane/protein systems, CG simulations have been used to predict the orientation of proteins in lipid bilayers,[16−20] the effect of hydrophobic mismatch on membrane/protein dynamics,[20−23] protein conformational changes,[24,25] and protein/protein interactions.[15,26] Thus, for certain applications, CG simulations can provide insights into systems and events that are out of reach of AT simulations.[8,27] CG simulations have also been used to perform more rigorous calculations such as, e.g., estimation of free energies of peptide/membrane interactions.[20,28−30] Although CG simulations can result in well sampled distributions, their ability to reproduce thermodynamic properties needs to be better evaluated.[31,32]

More recently, there has been interest in combining simulations performed at different levels of granularity.[33−36] One approach is to do this serially[34] where simulations at one level of granularity can be used to generate starting coordinates for simulations at a different level of granularity.[19,37] Simulations at one level of granularity can also be used to parametrize simulations at a different level of granularity.[33] Alternatively, one could do this in parallel where, e.g., a region of interest is described atomistically with the remainder of the system described with a CG model, with special treatments at the AT/CG boundary.[14,35,38]

We have recently used CG MD simulations to calculate the 1D potential of mean force (PMF) or free energy profile of a small peptide toxin interacting with a lipid bilayer via an umbrella sampling protocol.[20] The reaction coordinate corresponds to the position, projected along the bilayer normal (z axis), of the center of mass (com) of the toxin with respect to the com of the membrane. The toxin studied was VSTx1 (Voltage Sensor Toxin 1) from spider venom which inhibits the archeabacterial voltage-gated potassium (Kv) channel KvAP by interacting with the voltage-sensors.[39−42] Thus, VSTx1 inhibits KvAP by altering the energetics of voltage-dependent gating.[41,42] VSTx1 is a small globular protein (34 residues) with a distinct amphipathic molecular surface,[41−45] with one half of the toxin predominantly hydrophobic and the other half predominantly polar (Figure 1A). VSTx1 is positively charged (+3) at pH 7. It is structurally stable due to presence of 3 internal disulfide bridges.[46] Gating-modifier toxins such as VSTx1 gain access to the VS by first binding to the membrane/water interface.[41,42,44,47,48] Membrane partitioning is consistent with our CG free energy profiles which revealed a location at the membrane/water interface when VSTx1 interacted with lipid bilayers.[20] From a biophysical perspective, gating-modifier toxins such as VSTx1 have proved to be valuable characterization tools for studying voltage-gated ion channels.[41,42] From a computational point of view, the interaction of VSTx1 with lipid bilayers has been studied via CG[20] MD and via AT[49] MD simulations and is a tractable and well understood problem. It is therefore an ideal test system for a multiscale approach for computing the free energy of peptide/membrane interactions.

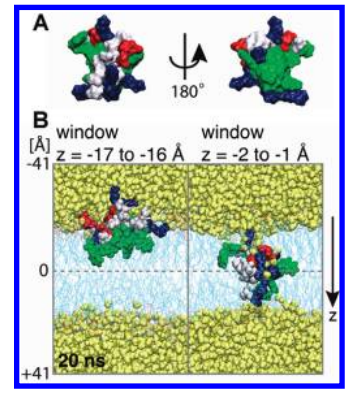

Figure 1. (A) VSTx1 has an amphipathic molecular surface with a hydrophilic (left) and a hydrophobic (right) side. Basic, acidic, polar, and hydrophobic residues of VSTx1 are colored blue, red, white, and green, respectively. (B) Atomistic (AT) umbrella sampling simulations were used to compute a 1D PMF profile where the reaction coordinate corresponds to the position, projected along the bilayer normal (z axis), of the center of mass (com) of the toxin with respect to the com of the membrane (the bilayer center is at $z \sim 0$ Å). A total of 82 umbrella sampling simulations or "windows" spaced 1 Å apart were used to sample from the extracellular (EC) solvent, across the bilayer, and into the intracellular (IC) solvent ($z = -41$ to $+41$ Å). Snapshots were taken at 20 ns for toxin locations at the free energy well at the bilayer/water interface ($z = -17$ to -16 Å; left) and in the hydrophobic core of the bilayer ($z = -2$ to -1 Å; right). POPC carbon, oxygen, nitrogen, and phosphorus atoms are colored cyan, red, blue, and gold, respectively, in a lines representation. Waters are colored yellow.

Here, we re-estimated the 1D PMF profile of VSTx1 interacting with a pure palmitoyl−oleoyl−phosphatidyl−choline (POPC) bilayer with *AT* simulations. An umbrella sampling protocol was used, and the reaction coordinate corresponds to the position, projected along the bilayer normal, of the com of the toxin with respect to the com of the membrane. The availability of considerable CG simulation data on this system (>30 μs[20]) permits a multiscale approach. We used the CG simulations to guide the setup of the AT simulations. Our motivation was to avoid local minima in the AT simulations, important for meaningful free energy estimates (see Theory and Methods), which is difficult to achieve over shorter AT time scales. As a further test, we used an implicit membrane/implicit solvent model[50] based on the generalized Born framework[51,52] (GBIM) to derive an estimate of a PMF profile where only the toxin was explicit. Cross-comparisons of the PMF profiles (AT, CG, and GBIM) revealed differences in the magnitude of the free energies although the overall topology of the landscapes was preserved. The PMF profiles reinforce the view whereby VSTx1 partitions from water into the membrane/water interface, with a considerable free energy barrier for positioning the toxin at the center of the membrane. By using

serial multiscale MD simulations, we have obtained a unified view of how VSTx1 interacts with a membrane.

Theory and Methods

Umbrella Sampling MD Simulations to Derive a Potential of Mean Force Profile. The PMF $W(\varepsilon)$ along a reaction coordinate ε is the constrained free energy and can be defined from the average distribution $\langle\rho(\varepsilon)\rangle$

$$W(\varepsilon) = W(\varepsilon^*) - k_B T \ln\left[\frac{\langle\rho(\varepsilon)\rangle}{\langle\rho(\varepsilon^*)\rangle}\right]$$

where ε^* and $W(\varepsilon^*)$ are arbitrary constants.[53] The average distribution function along the coordinate ε is obtained from a Boltzmann weighted average

$$\langle\rho(\varepsilon)\rangle = \frac{\int \delta(\varepsilon'[R] - \varepsilon) e^{-U(R)/k_B T}\, dR}{\int e^{-U(R)/k_B T}\, dR}$$

where $U(R)$ represents the total energy of the system as a function of the coordinates R, and $\varepsilon'[R]$ is a function depending on one or more degrees of freedom in the system.[53]

MD simulations can be used to sample $\langle\rho(\varepsilon)\rangle$. However, the presence of energy barriers along ε, together with simulations of finite duration, are likely to prevent adequate sampling of $\langle\rho(\varepsilon)\rangle$. With umbrella sampling MD simulations, one performs an ensemble of N biased simulations or "windows" where an external biasing potential $\omega(\varepsilon)$ is applied to force the system to sample over the range of interest along ε. Each window samples the neighborhood of a chosen value of ε, and one obtains N biased distributions which need to be unbiased and combined to obtain a single unbiased distribution.[53,54] In the current study, we used the weighted histogram analysis method (WHAM).[55] We emphasize that the integral in the average distribution function implies that all nonsampled degrees of freedom "perpendicular" to the reaction coordinate ε must equilibrate in *all* windows before collecting distributions along ε for the PMF to be meaningful.

Serial Multiscale CG and AT Simulations. MD simulations[18,20,49] and experiments[41,56] suggest VSTx1 and related gating-modifier toxins have a distinct orientation when bound to the lipid bilayer. At its optimal location of interaction at the membrane/water interface, the polar residues of VSTx1 are directed toward solvent where they interact with the lipid headgroups, with the hydrophobic residues exposed to the lipid tails (Figure 1B; left panel).[20] To obtain a meaningful PMF profile, it is crucial that the orientation of VSTx1 equilibrates at each point along the reaction coordinate z (the z axis corresponds to the bilayer normal). This was achieved in our recent CG free energy simulations.[20] We had used 104 independent CG windows (each of duration 40 ns) spaced 1 Å apart along z to sample configurations of VSTx1 from the extracellular (EC) solvent, across a POPC bilayer, and into the intracellular (IC) solvent. An *identical* initial orientation of the toxin relative to the bilayer was used in all windows (as shown in Figure 2A; 0 ns). We quantified the orientation of VSTx1 by the angle of its hydrophobic moment (defined as the vector sum of the hydrophobicity of each constituent residue of a peptide[57]) relative to the bilayer normal (θ; Figure 2A; note that θ ranges from 0° to 180°). θ equilibrated by 20 ns for CG windows where VSTx1 interacted with the bilayer to effectively minimize the hydrophobic mismatch between the toxin and its environment (Figure 2B). Thus, a distinct toxin orientation as a function of z exists. The only exceptions were windows where the toxin was located in water, away from the bilayer. Here, VSTx1 tumbled randomly in water.

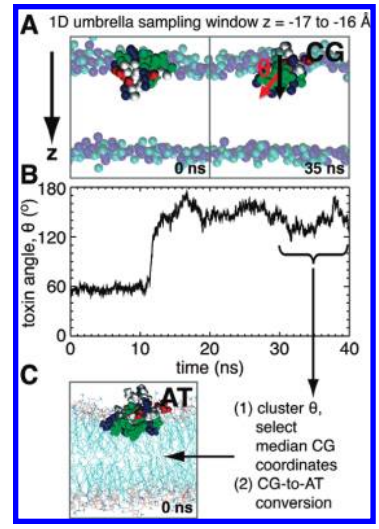

Figure 2. Serial multiscale CG[20] and AT umbrella sampling simulations. (A, B) An identical initial orientation of VSTx1 (relative to the membrane) was previously used for all CG windows (window z = 16 to 17 Å shown; each CG window was simulated for 40 ns).[20] The orientation of VSTx1 (as defined by the angle of the hydrophobic moment of the toxin[57] θ) relative to the bilayer normal equilibrated by 20 ns in all windows. (C) Each CG window was clustered on the backbone of VSTx1 and over the final 10 ns (i.e., 30 to 40 ns/window; after toxin orientation had equilibrated). The median of the cluster, which corresponds to the system with the most frequently observed equilibrated orientation of VSTx1, was used to guide the setup of the corresponding AT window. POPC phosphates and cholines are colored blue and cyan, respectively, in the CG snapshots. All other CG particles were not shown for clarity.

To set up the AT umbrella sampling simulations, we clustered each CG window on the backbone of VSTx1 and over the final 10 ns (i.e., 30 to 40 ns/window; after toxin orientation had equilibrated) using the full linkage algorithm.[58] The median of the cluster, which corresponds to the system with the most frequently observed equilibrated orientation of VSTx1, was selected. The NMR structure of VSTx1[44] was least-squared-fitted on the CG toxin coordinates, and the AT toxin was subsequently modeled into an AT POPC bilayer (Figure 2C; see Umbrella Sampling MD Simulation Setup).

Thus, unlike the CG free energy simulations where an arbitrary initial orientation of VSTx1 was used in each window,[20] knowledge gained from the CG simulations was used to initiate the orientation of the toxin in the AT free energy simulations. We therefore assumed (i) the orientation of VSTx1 relative to the bilayer was the overwhelming factor

that would have influenced the accuracy of a 1D PMF along z, and (ii) the CG model[59] was able to predict θ accurately. The latter is reasonable as, e.g., the CG model has successfully predicted the insertion and orientation of a range of membrane/membrane-associated proteins in lipid bilayers[16−18] including VSTx1.[20]

Umbrella Sampling MD Simulation Setup. To perform AT umbrella sampling, we used 82 windows along z spaced 1 Å apart ($z = -41$ to 41 Å; the bilayer center is at $z \sim 0$ Å; Figure 1B) to sample from the EC solvent, across the bilayer, and into the IC solvent. For each window, 20 ns AT MD simulation was employed. In total, we accumulated >1.6 μs of AT MD simulation data. The z coordinate of the com of VSTx1 was restrained relative to the z coordinate of the com of the entire bilayer with a harmonic biasing potential (e.g., in window $z = -41$ to -40 Å, the com of VSTx1 was restrained at -40.5 Å relative to the com of the bilayer). We used a pre-equilibrated POPC bilayer containing 128 lipids (courtesy of Peter Tieleman; moose.bio.ucalgary.ca). To generate initial coordinates for VSTx1 in the bilayer, we used a protocol similar to that employed in previous simulations of VSTx1[20,49] and related toxins.[18] Briefly, we modeled VSTx1 in the bilayer by gradually scaling the coordinates of the toxin to its full size in 10 steps, with 100 steps of steepest-descent energy minimization at each step to allow the lipids to adjust their conformations to host the toxin. The intramolecular interactions (i.e., interactions between the atoms of VSTx1) were switched off; however, interactions between VSTx1 and the lipids remained. The lipid coordinates from each previous step were kept while the original toxin coordinates were rescaled. At each step, any lipid whose phosphorus atom was within 2.5 Å of any toxin atom was removed. A cutoff of 2.5 Å was found to be optimal for removing steric clashes between VSTx1 and the lipids, while ensuring the lipids were adequately packed around the toxin. Across all windows, no more than 7 lipids/window were removed.

We had previously constrained our CG free energy simulations of VSTx1 interacting with a membrane by limiting excessive membrane deformation, to study the effects of membrane deformability on free energies.[20] We used a similar setup in our AT free energy simulations. Thus, positional restraints where applied on the phosphorus atoms of all lipids along the bilayer normal z.

AT umbrella sampling MD simulations were performed using GROMACS 3.2.1 (www.gromacs.org)[60,61] using the GROMOS-96 force-field[62] and Berger parameters for POPC lipids.[63,64] VSTx1 was kept in the default protonation state for pH 7. Each system was solvated with SPC waters.[65] Cl^- counterions were added to keep each system electrically neutral. Long-range electrostatic interactions were calculated using the particle mesh Ewald (PME) method,[66] employing a grid spacing of ~ 1 Å^{-1} and an interpolation order of 4. A cutoff of 12 Å was used for the real space portion of the Ewald sum and the Lennard-Jones interactions. The LINCS algorithm[67] was applied to constrain all covalent bonds, and the SETTLE algorithm[68] was used to maintain the geometry of the water molecules. Each system was temperature coupled with a Berendsen thermostat[69] with a weak coupling constant of 0.1 ps and a reference temperature of 310 K. Semi-isotropic pressure coupling with a Berendsen barostat in x and y at 1 bar with a coupling constant of 1.0 ps and a compressibility value of 4.6×10^{-5} bar^{-1} was used. Prior to production, a short MD simulation of duration 0.5 ns/window (with positional restraints applied on the toxin, and on the phosphorus atoms of the lipids in z only) was performed to allow the lipids to further repack around the toxin, and to allow the waters and counterions to settle. This was followed by a production simulation of duration 20 ns/window. The time step of integration was 2 fs. Positional restraints and the biasing potential utilized a force constant of 10 kJ mol^{-1} Å^{-2}. All simulations utilized a TM voltage of 0 V. The biased probability distributions were combined and unbiased with an implementation of WHAM[55] (courtesy of Alan Grossfield; membrane.urmc.rochester.edu), using 100 bins over -41 Å and $+41$ Å and a tolerance of 0.0001.

The Generalized Born Membrane. The generalized Born implicit membrane (GBIM) used here has been described in detail in a previous publication.[70] In brief, the membrane is modeled as a low dielectric zone in a uniform aqueous implicit solvent (with a dielectric constant $\epsilon_{water} = 80$). The zone has a Gaussian cross-section becoming increasingly inaccessible to the solvent toward its center. Both the protein interior and the membrane are assumed to have the same interior dielectric constant of $\epsilon_{membrane} = 2$. The Born radii were calculated using the fast asymptotic pairwise summation, using the original OPLS all atom parametrization by Qiu and Still.[71] This yields excellent results in predicting experimental free energies of solvation as well as hydration effects on conformational equilibria.[72] The membrane was introduced by modifying the pairwise summation to solute atoms, the self-solvation terms $\Gamma(z_i, L)$, and the atomic volumes $V(z_i)$, which were made to vary smoothly between full solvation and a limiting value for burial at the center of the membrane. A Gaussian shape

$$\Gamma(z_i) = g_{bulk} + (g_{centre} - g_{bulk})\, e^{\gamma(z_i^2/L^2)}$$

was used, where g_{bulk} is the limiting value of Γ at a large distance from the membrane (i.e., $z \gg L$) corresponding to the self-solvation term of the unmodified generalized Born method, while g_{center} is the value of Γ at the membrane center. We used a Gaussian with $\gamma = -3.0$ and membrane half width of $L = 15$ Å, which corresponds roughly to the hydrophobic profile of a dipalmitoyl−phosphatidyl−choline (DPPC) lipid bilayer. A value of $g_{center} = -7.67$ kcal/mol was used, as reported previously.[73,74] Gaussians were chosen in good agreement with experimental evidence from lipid distortion[75,76] and X-ray and neutron diffraction experiments on fluid liquid-crystalline bilayers.[77] The OPLS-AA force field[78] was used to describe the toxin.

The nonpolar part of the solvation free energy is modeled using an effective surface tension associated with the solvent accessible surface area (SA).[71] As it is moved toward the center of the membrane, the surface energy contribution of each atom is scaled down by an exponential switch at the membrane interface ($z = \pm 15$ Å). Thus, for distances far from the membrane (i.e., $z \gg L$), the nonpolar contribution

is included with the positive surface tension of solvation in water, while in the center of the membrane the surface tension is negative (i.e., energy is gained by moving into the membrane from the gas phase), as determined experimentally.[79]

Calculating the Minimal Energy Conformation to Derive a Potential of Mean Force Profile. The minimal energy configuration of VSTx1 in a GBIM membrane was calculated by exploring the entire translational and rotational space of VSTx1 in the membrane, treating the toxin as a rigid body. Previous AT simulations of VSTx1 in water and lipid bilayers[49] revealed the toxin to be conformationally stable, with little structural drift from the initial toxin conformation over multinanosecond time scales, and no unfolding. The principal axis of the toxin was determined through diagonalization of the inertia tensor using only the heavy backbone atoms. The tilt angle was defined as the angle of the principal axis with respect to the membrane normal, while the rotation angle was defined as the angle of rotation around the principal axis.

The toxin was translated from $z = -50$ Å to $+50$ Å along the membrane normal (membrane center = 0 Å) in 0.5 Å steps. At each step, the toxin was rotated through all space to find the orientation of minimum energy by first tilting it with respect to the membrane normal and subsequent rotation around its principal axis until all tilt and rotational states have been sampled with a step size of 1°. The lowest energy conformation encountered was then subjected to a rigid body minimization in order to locate the precise location of the global energy minimum. Because the membrane and solvent are implicit (i.e., always at equilibrium) and VSTx1 is treated as a rigid body (which is not unreasonable as the toxin is conformationally stable), the potential energies approximate to free energies. Thus, for this system, the GBIM rigid body scan provides a reasonable approximation of a free energy surface. We do not expect the GBIM profile to differ significantly had we used GROMOS-96 instead of the OPLS-AA force field to describe the toxin in the rigid body scan.

Results

Toxin Structures in the AT MD Free Energy Simulations. We monitored the structural stability of VSTx1 by calculating the root-mean-squared-deviation (RMSD) of the C_α atoms of the toxin with respect to the initial toxin structure (after a C_α least-squared-fit; Figure S1, Supporting Information). For the majority of the windows, the RMSDs did not exceed 3.5 Å. The only exceptions were toxin locations in water furthest away from the bilayer ($z = -41$ to -39 Å and $z = 39$ to 41 Å) and several toxin locations close to the center of the hydrophobic core of the bilayer ($z = -8$ to -7 Å, $z = 1$ to 3 Å and $z = 4$ and 5 Å) where the RMSDs approached 4 to 5 Å. In the water, VSTx1 experienced a larger conformational drift compared to the ordered lipid environment. For toxin locations close to the center of the hydrophobic core of the bilayer, VSTx1 optimized the interaction of its polar residues with the lipid headgroups resulting in an increase in RMSDs (discussed further below). In all windows, the toxin remained globular and did not unfold. Ignoring the N-terminal residue and the two C-terminal residues of VSTx1 which are flexible,[49] the RMSDs did not exceed 3.5 Å in *any* window (Figure S2, Supporting Information).

We investigated the time-averaged root-mean-squared-fluctuations (RMSF) of the C_α atoms of the toxin with respect to the initial toxin structure (Figures S3 and S4, Supporting Information). It can be seen that the residues near the N- and C-termini (i.e., E1, P33, and F34) had RMSFs approaching and exceeding 3 Å. Consistent with previous AT simulations,[49] four distinct regions with low RMSFs of 0.3 to 1.0 Å were observed between residues 2 and 9, 14 and 16, 19 and 22, and 27 and 30 due to the presence of 3 internal disulfide bridges (between C2 and C16, C9 and C21, and C15 and C28) and 2 β-strands. Consistent with the RMSDs, VSTx1 exhibited greater conformational flexibility in water compared to when buried in the bilayer. The overall pattern of flexibility is consistent with the presence of secondary structure elements and disulfide bridges in the toxin.

Comparison of CG and AT Umbrella Sampling Simulations. We compared the orientation of VSTx1 θ of each AT window vs the corresponding CG window.[20] Figure 3A−C show the distribution of the angle of the hydrophobic moment of the toxin (relative to the bilayer normal; θ) of the AT windows (over 17 to 20 ns; discarding the initial 17 ns as equilibration time) compared with the distributions obtained from the corresponding CG windows (over the final 10 ns, i.e., 30 to 40 ns; after the orientation of VSTx1 had equilibrated).[20] We show this for three windows: (i) with VSTx1 located in water ($z = -41$ to -40 Å; where the com of VSTx1 was restrained at -40.5 Å relative to the com of the bilayer), (ii) with VSTx1 located at the free energy well at the membrane/water interface ($z = -17$ to -16 Å; discussed below), and (iii) with VSTx1 buried close to the center of the hydrophobic core of the bilayer ($z = -2$ to -1 Å).

In water, θ distributions were broad in both CG and AT windows compared to toxin locations in the bilayer, between 40° and 155°. Thus, VSTx1 exhibited greater orientational freedom in water as it tumbled randomly under the influence of the solvent molecules. At the membrane/water interface ($z = -17$ to -16 Å), θ fluctuated over a smaller range of 30° (i.e., between 150° and 180°) in both CG and AT windows. A good overlap can be seen between CG and AT distributions, and θ had an average (± 1 SD) of 168° ± 6° (CG; averaged over 30 to 40 ns) and 168° ± 3° (AT; averaged over 17 to 20 ns), respectively. In this orientation, the polar and hydrophobic residues of VSTx1 were optimally located to interact with the lipid headgroup and tails respectively.

With the toxin buried in the hydrophobic core of the bilayer ($z = -2$ to -1 Å), the CG and AT θ distributions did not overlap; θ had an average of 142° ± 8° and 89° ± 7° in the CG and AT windows, respectively. Inspection of CG window $z = -2$ to -1 Å showed VSTx1 adopted an orientation such that the polar residues of the toxin were positioned to interact with the lipid headgroups of the EC leaflet. Thus, at 0 ns, VSTx1 had a similar orientation in the corresponding AT window (Figure 3C; see inset). Over 20

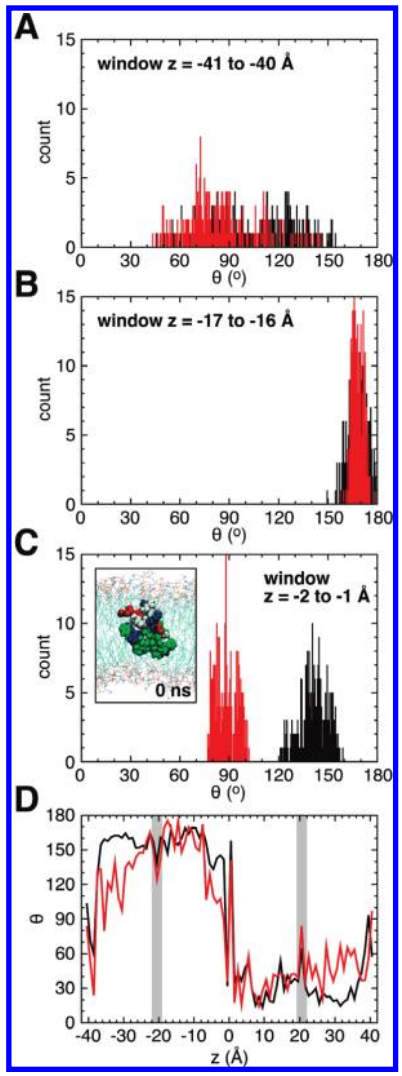

Figure 3. Toxin orientation in the CG and AT simulations. The distributions of the angle of the hydrophobic moment of VSTx1 (relative to the bilayer normal; θ) are shown for CG[20] (black) and AT (red) umbrella sampling windows: (A) $z = -41$ to -40 Å, (B) $z = -17$ to -16 Å, and (C) $z = -2$ to -1 Å. The inset figure in C shows the AT system at 0 ns. (D) Average of θ ($\bar{\theta}$) as a function z for the CG and AT simulations. Averages and distributions are over 30 to 40 ns and 17 to 20 ns per CG and AT window, respectively. The gray regions in D indicate the approximate location of the lipid phosphates.

ns of AT MD, VSTx1 reorientated such that its polar residues were positioned to interact with the lipid headgroups of *both* EC and IC leaflets, accompanied by penetrating water molecules "shielding" the polar residues from the hydrophobic lipid tails. Thus, the hydrophobic surface of VSTx1 was directed perpendicular to the bilayer normal (Figure 1B; right panel). This toxin orientation is possible as VSTx1 was approximately equidistant from the lipid headgroups of both leaflets. Encouragingly, this suggests that 20 ns is sufficient to allow for optimization of the orientation of the toxin in the lipid bilayer in the AT simulations. Thus, the AT simulations showed another mode of interaction of VSTx1 with a POPC bilayer which was not observed in the CG simulations.

In Figure 3D, we plot the average of θ ($\bar{\theta}$) as a function of z in the CG and AT windows. Averages were calculated over 30 to 40 ns and 17 to 20 ns per CG and AT window, respectively. Two distinct values of $\bar{\theta}$ are observed from $z \sim -35$ to 35 Å in the CG simulations: ~155° from $z \sim -35$ to -3 Å and ~25° from $z = 0$ to 35 Å. Thus, VSTx1 underwent a ~180° "flip" as it crossed the bilayer center to minimize the hydrophobic/hydrophilic mismatch between itself and the environment.[20] The "flip-flop" transition in $\bar{\theta}$ between $z \sim -3$ and 0 Å was because chance dictated whether the polar residues of VSTx1 would interact with the headgroups of the EC or IC leaflet. With the toxin located in water in the CG simulations (i.e., $z \sim -41$ to -35 Å and $z \sim 35$ to 41 Å), the SD of θ approached 37° corresponding to VSTx1 tumbling freely in water, compared to SD values of <14° between $z = -35$ and 35 Å when the toxin interacted with the membrane.

In the AT simulations toward water, a somewhat earlier (at $z \sim \pm 25$ Å) and more gradual drift in $\bar{\theta}$ away from the plateau can be seen because of the finer resolution (i.e., more rugged energy landscape) afforded by the AT simulations. We anticipate directionality offered by H-bonding interactions (between VSTx1 and the membrane) in the AT simulations to fine-tune the orientation of the toxin. Between $z \sim -7$ and $+7$ Å with VSTx1 buried in the bilayer, there are clear deviations in the orientation of the toxin over 20 ns, and the difference in $\bar{\theta}$ between the AT and corresponding CG windows was >50°. Thus, between $z = -7$ and $+7$ Å, VSTx1 reorientated such that its polar residues interacted with the lipid headgroups of both EC and IC leaflets. Interaction of the polar residues of Hanatoxin (HATx), a related gating-modifier toxin with an amphipathic molecular surface, with the lipid headgroups of both leaflets, has been reported in recent AT simulations of HATx interacting with a DPPC bilayer.[80] Although our free energy profiles (discussed below) suggest such a mode of interaction is unlikely given the interfacial free energy wells, at least when VSTx1 interacts solely with the bilayer, this may not be physiologically irrelevant when VSTx1 (and other gating-modifier toxins) interacts with both the membrane and the VS of Kv channels.[41,42,47] Overall, $\bar{\theta}$ in the AT simulations correlates with the CG simulations. Taken together, this suggests the CG simulations can be used to guide the setup of the AT simulations, and deviations from the initial AT setup are still permissible (as observed in a few windows with the toxin near the bilayer center) over the time-course of the AT simulations (20 ns).

Free Energy Profiles from Umbrella Sampling MD Simulations. The AT and CG[20] PMF profiles in Figure 4 depict the free energy cost of positioning VSTx1 at different depths in a POPC bilayer. Block analyses (the distributions are split into nonoverlapping blocks to derive multiple PMF profiles in order to evaluate convergence) suggest the AT profile had sufficiently converged (Figure S5, Supporting Information). The AT profile had free energy wells at the membrane/water interface at ~±13 to 18 Å, which was somewhat closer to the bilayer center than the CG profile (~±22 Å).[20] The shift in the location of the interfacial minima by ~5 Å between the CG and AT profiles can be accounted for by differences in the equilibrium thickness of the CG and AT membranes and is not due to differences in

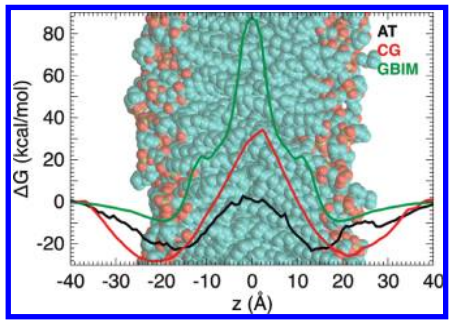

Figure 4. PMF profiles for positioning VSTx1 at different depths in a POPC bilayer. A snapshot of a POPC bilayer is shown in the background for reference. The PMFs shown are derived from AT umbrella sampling simulations (black line), from CG umbrella sampling simulations (red line),[20] and from a rigid body scan of VSTx1 with an implicit solvent and membrane model (GBIM; green line). Because membrane and solvent are implicit and VSTx1 is assumed to be rigid, the GBIM rigid body scan provides a reasonable approximation of a free energy profile. The bilayer center is at $z \sim 0$ Å.

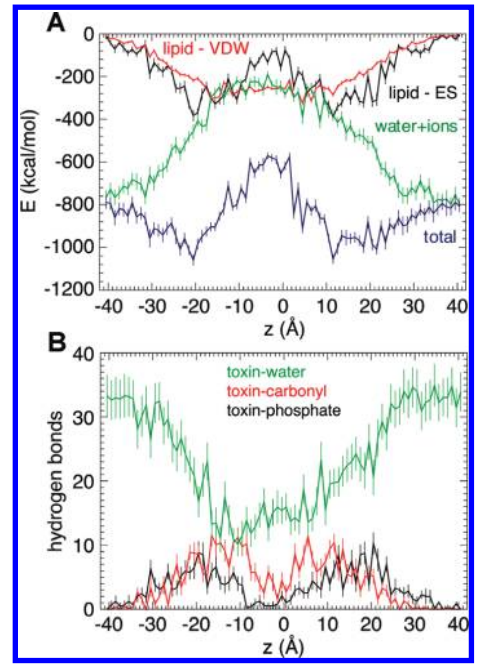

Figure 5. VSTx1/environment interactions in the AT simulations. (A) Toxin−environment interaction (i.e., potential) energies (IE). Average toxin−lipid, toxin−solvent, and total toxin−environment (i.e., toxin−lipid + toxin−solvent) IE. The toxin−lipid IE was decomposed into electrostatic (ES) and VDW components. (B) Hydrogen bonding (H-bonding) interactions. Average number of H bonds between VSTx1 and waters, POPC carbonyls, and POPC phosphates. Averages were taken over 17 to 20 ns/window. Bars represent ±1 SD.

the way VSTx1 interacted with the bilayer. The AT well was −23 kcal/mol (with respect to water), while the central barrier at ∼0 Å was +26 kcal/mol (with respect to the interfacial well). We note the AT profile was not symmetrical about the bilayer center (i.e., $z = 0$ Å). When modeling VSTx1 in the bilayer, we had to remove a few lipids to accommodate the toxin, and this had resulted in asymmetric bilayers (i.e., a bilayer with different numbers of lipids in each leaflet; Figure S6, Supporting Information) and could have contributed to the asymmetry in the free energy profile. Overall, the AT profile suggests it is energetically favorable for VSTx1 to partition into the headgroup/tail interface of a POPC bilayer than to remain in water, and we do not expect the toxin to be able to cross the width of the membrane, consistent with experimental data.[41,42]

Although the topology of the AT and CG profiles was conserved, there were differences in the magnitude of the free energies. The AT and CG free energy wells at the interface were somewhat comparable and differed by ∼4 kcal/mol (−23 vs −27 kcal/mol for AT and CG, respectively). However, the central barrier differed by 36 kcal/mol (+26 vs +61 kcal/mol for AT and CG, respectively, with respect to the well). With VSTx1 buried in the bilayer, water molecules penetrated into the hydrophobic membrane core to provide a micropolar environment for the polar residues of the toxin (Figure 1B, right panel). Water penetration was observed to a more limited extent in the CG simulations.[20] Furthermore, as the polar residues of VSTx1 interacted with the lipid headgroups of both EC and IC leaflets with the toxin buried in the bilayer, this would further stabilize the toxin at the center of the membrane. Taken together, these could account for the increased CG central barrier.

An Approximation of a Free Energy Profile from the Generalized Born Implicit Membrane Model. Although approximate, an implicit membrane and solvent approach allows one to quickly ascertain the topology of the energy landscape and provides a further test of the predicted AT and CG MD PMF profiles. The GBIM rigid body scan provides a reasonable approximation of a free energy profile because membrane and solvent are implicit and VSTx1 is assumed to be rigid. In Figure 4, a free energy well of 9 kcal/mol (with respect to water) was present at ±20 Å, and we observed a central barrier of 97 kcal/mol (with respect to the interfacial well). Thus, the GBIM free energy well was reduced compared to the AT and CG profiles (i.e., −9 vs −23 vs −27 kcal/mol for GBIM, AT, and CG, respectively). The membrane/water interface provides a unique and complex hydrogen bonding (H-bonding) environment that is not sufficiently modeled by an implicit membrane/solvent approach. Enthalpic contributions from H-bonds (i.e., relatively strong electrostatic interactions) between VSTx1, and the lipid phosphate and glycerol moieties (ref 49, and discussed below) at the interface could be significant. Possible water defects in the membrane are modeled to a different extent in the three approaches (i.e., AT, significant; CG, limited; and GBIM, absent), which may explain the differences in the magnitude of the central barrier (i.e., 97 vs 26 vs 61 kcal/mol for GBIM, AT, and CG, respectively). We do not expect the GBIM-derived PMF profile to be very different had we accounted for the internal dynamics of VSTx1 as the toxin has a stable fold.

Toxin-Environment Interaction Energies and Hydrogen Bonding Interactions. To gain a better insight into the nature of the interactions that stabilize VSTx1 in a lipid bilayer environment, we investigated the average interaction (i.e., potential) energies (IE) between the toxin and its environment in the AT simulations. In Figure 5A, we plot

the average toxin−lipid and toxin−solvent IE (averaged over 17 to 20 ns/window) as a function of z, together with the average total toxin−environment IE (i.e., toxin−lipid IE + toxin−solvent IE). The toxin−lipid IE was decomposed into electrostatic (ES) and van der Waals (VDW) components. Only the real space component of PME is reported for the toxin−lipid ES component. The VDW component of the toxin−lipid IE increased (i.e., became more negative) with increased VSTx1 exposure to the membrane towards 0 Å. The ES component of the toxin−lipid IE dictated the topology of the total toxin−environment IE profile. This is consistent with previous AT simulations of VSTx1 with lipid bilayers where ES interactions between the basic residues of the toxin (K4, K8, K10, K17, R24, and K26) and the negatively charged lipid phosphates were important for stabilizing the toxin in the membrane.[49] The toxin−solvent IE is not zero with VSTx1 located at the bilayer center (i.e., at $z = 0$ Å). As discussed earlier, a combination of toxin reorientation, toxin structural drift (as shown by the RMSDs), and penetration of waters ensured continued interaction between VSTx1 and solvent even when the toxin was completely buried in the membrane (Figure 1B, right panel).

In Figure 5B, we investigate H-bonding interactions between VSTx1 and its environment (i.e., waters, lipid carbonyls, and lipid phosphates) in the AT simulations. We plot the average number of H bonds over 17 to 20 ns/window. The toxin−phosphate H bonds had a maximum of 11 at $z \sim \pm 20$ Å, and the toxin−carbonyl H bonds had a maximum of 12 at $z \sim \pm 15$ Å, consistent with the location of the different lipid moieties along the bilayer normal. VSTx1 formed up to 17 hydrogen bonds with waters between $z = -5$ and 5 Å (i.e., when the toxin was located close to the bilayer center). In going from water to the membrane, the loss of H bonds with waters (from, e.g., ∼34 H bonds at ±40 Å) is compensated for by the formation of H bonds with lipids. Indeed, the maximum *total* (i.e., with waters and lipids) number of H bonds is formed when VSTx1 is located at the membrane/water interface at ∼20 Å where, additionally, the hydrophobic residues of the toxin can find a favorable environment as they were directed at the lipid tails. This is consistent with the location of the free energy wells in the PMF profiles. Thus, the free energy of desolvation of the hydrophobic residues of VSTx1 is likely to be a major contributor to the interfacial free energy wells.

Discussion and Conclusion

We have combined CG and AT simulations serially to compute a 1D PMF (i.e., free energy) profile for the interaction of a small protein with a lipid bilayer. We used information gained from CG free energy simulations[20] to guide the setup of corresponding AT simulations. We calculated the 1D free energy profile of VSTx1 interacting with a POPC bilayer, where the reaction coordinate corresponds to the position, projected along the bilayer normal, of the com of the toxin with respect to the com of the membrane. The VSTx1/bilayer system was chosen as a test system for multiscale analysis of protein/membrane interactions as it is reasonably simple and well characterized.[20,41,42,49] How VSTx1 interacts with membranes is also of interest in the context of the biophysics of voltage sensing by potassium channels.[41,42,47,81−83] The interaction of VSTx1 with a bilayer will also provide insights into how small amphipathic proteins and peptides interact with lipid bilayers. From a theoretical point of view, in a 1D PMF of VSTx1 along the membrane normal z, there is an important nonsampled degree of freedom that had to equilibrate in order to yield meaningful PMFs. The important nonsampled degree of freedom is due to the amphipathic surface of VSTx1, giving the toxin a distinct orientation as a function of position in the bilayer. The longer time scales accessible to CG simulations allowed the toxin orientation to equilibrate. The initial AT configurations were based on the equilibrated CG configurations, and the AT simulations provided a finer view of how VSTx1 interacted with the membrane.

The CG and AT PMF profiles had a conserved topology (i.e., interfacial wells and a central barrier), but there were differences in the magnitude of the free energies. The interfacial free energy wells are comparable (i.e., −27 vs −23 kcal/mol for CG and AT, respectively), which remains considerably larger than that derived experimentally for VSTx1 (−7 kcal/mol[48]) and related gating-modifier toxins that target the VS of Kv channels (−3.5 to −8.5 kcal/mol[84]). With VSTx1 located close to the interfacial well, e.g., in AT window $z = -17$ to -16 Å, the com of L30 of the toxin, centered on the hydrophobic patch, was positioned at a distance of ∼10 Å from the bilayer center, which is in agreement with depth-dependent fluorescence quenching data on HATx (W30 of HATx1 was reported to be positioned at a distance of 9 Å from the membrane center).[47] The largest difference between the CG and AT profiles was the central barrier (61 vs 26 kcal/mol for CG and AT, respectively). This difference may be accounted for by phenomena observed in the AT simulations which were absent or observed to a limited extent in the CG simulations: (1) water defects in the membrane (which were more limited in the CG simulations because of the lack of dipoles in CG waters[7]) and (2) when displaced toward the membrane center, VSTx1 reorientated such that its polar residues interacted with the lipid headgroups of *both* leaflets, consistent with simulations of a related toxin[80] (this was not observed in the CG simulations[20]). We emphasize that this 1D PMF profile would be difficult to compute using AT simulations in isolation, without guidance from CG simulations, because of likely problems with sampling and convergence.

To illustrate this, we performed additional simulations of VSTx1 located at the interfacial free energy well but in a nonoptimal initial orientation (i.e., "upside-down" relative to the bilayer; Figure S9, Supporting Information). The toxin would require well in excess of 20 ns to locate its optimal orientation in the bilayer. It would therefore be difficult to compute this PMF, using an AT force-field, without *a priori* knowledge of toxin orientation as a function of reaction coordinate z.

Despite the CG bias, for a few toxin locations close to the bilayer center that we observed, VSTx1 was able to deviate substantially from its initial orientation in the AT simulations to adopt configurations which were not observed in the CG simulations. Thus, the AT simulations could

sample new configurations of toxin orientation. Taken together, it is clear a serial multiscale approach has allowed for better estimates of this PMF profile. One could also combine the multiscale procedure presented here with other enhanced sampling methods (e.g., hybrid Monte Carlo[85] or replica exchange[86]) to achieve further exploration of the AT energy landscape.

The AT simulations provided insights into how lipids might interact with gating-modifier toxins such as VSTx1 when they are located at their optimal binding depth in lipid bilayers. The lipids were seen to "wrap" their acyl chains around the hydrophobic face of VSTx1 (Figure S8, Supporting Information).

Returning to a more biological perspective, it is of interest that recent experimental studies of the action of VSTx1 on Kv channels have been interpreted in terms of perturbation of membrane/channel forces by the toxin.[82] Thus, a detailed understanding of the nature and location of the toxin/bilayer interaction becomes crucial to our understanding of the mode of action of the toxin. The multiscale procedure presented here provides a valuable tool for such studies.

Acknowledgment. We thank our colleagues in the Structural Bioinformatics and Computational Biochemistry Unit, in particular Ranjit Vijayan, for their helpful comments. C.L.W. is funded by the Oxford Centre for Integrative Systems Biology (OCISB). Research in M.S.P.S.'s laboratory is funded by BBSRC and the Wellcome Trust. We acknowledge the U.K. National Grid Service for computing resources.

Supporting Information Available: Additional analyses of the simulations described in this paper. This information is available free of charge via the Internet at http://pubs.acs.org/.

References

(1) Rodinger, T.; Pomès, R. Enhancing the accuracy, the efficiency and the scope of free energy simulations. *Curr. Opin. Struct. Biol.* **2005**, *15*, 164–170.

(2) Allen, T. W.; Andersen, O. S.; Roux, B. Energetics of ion conduction through the gramicidin channel. *Proc. Natl. Acad. Sci. U.S.A.* **2004**, *101*, 117–122.

(3) Bernèche, S.; Roux, B. Energetics of ion conduction through the K^+ channel. *Nature* **2001**, *414*, 73–77.

(4) Hub, J. S.; de Groot, B. L. Mechanism of selectvity in aquaporins and aquaglyceroporins. *Proc. Natl. Acad. Sci. U.S.A.* **2008**, *105*, 1198–1203.

(5) Pongprayoon, P.; Beckstein, O.; Wee, C. L.; Sansom, M. S. P. Simulations of anion transport through OprP reveal the molecular basis for high affinity and selectivity for phosphate. *Proc. Natl. Acad. Sci. U.S.A.* **2009**, *106*, 21614–21618.

(6) MacCallum, J. L.; Bennett, W. F. D.; Tieleman, D. P. Distribution of amino acids in a lipid bilayer from computer simulations. *Biophys. J.* **2008**, *94*, 3393–3404.

(7) Marrink, S. J.; de Vries, A. H.; Mark, A. E. Coarse grained model for semiquantitative lipid simulations. *J. Phys. Chem. B* **2004**, *108*, 750–760.

(8) Nielsen, S. O.; Lopez, C. F.; Srinivas, G.; Klein, M. L. Coarse grain models and the computer simulation of soft materials. *J. Phys.: Condens. Matt.* **2004**, *16*, R481–R512.

(9) Izvekov, S.; Voth, G. A. A multiscale coarse-graining method for biomolecular systems. *J. Phys. Chem. B* **2005**, *109*, 2469–2473.

(10) Shi, Q.; Izvekov, S.; Voth, G. A. Mixed atomistic and coarse-grained molecular dynamics: simulation of a membrane bound ion channel. *J. Phys. Chem. B* **2006**, *110*, 15045–15048.

(11) Shih, A. Y.; Arkhipov, A.; Freddolino, P. L.; Schulten, K. Coarse grained protein-lipid model with application to lipoprotein particles. *J. Phys. Chem. B* **2006**, *110*, 3674–3684.

(12) Bond, P. J.; Holyoake, J.; Ivetac, A.; Khalid, S.; Sansom, M. S. P. Coarse-grained molecular dynamics simulations of membrane proteins and peptides. *J. Struct. Biol.* **2007**, *157*, 593–605.

(13) Marrink, S. J.; Risselada, J.; Yefimov, S.; Tieleman, D. P.; de Vries, A. H. The MARTINI forcefield: coarse grained model for biomolecular simulations. *J. Phys. Chem. B.* **2007**, *111*, 7812–7824.

(14) Voth, G. A. *Coarse-Graining of Condensed Phase and Biomolecular Systems*; CRC Press: Boca Raton, FL, 2008.

(15) Periole, X.; Cavalli, M.; Marrink, S. J.; Ceruso, M. A. Combining an elastic network with a coarse-grained molecular force field: structure, dynamics, and intermolecular recognition. *J. Chem. Theory Comput.* **2009**, *5*, 2531–2543.

(16) Scott, K. A.; Bond, P. J.; Ivetac, A.; Chetwynd, A. P.; Khalid, S.; Sansom, M. S. P. Coarse-grained MD simulations of membrane protein-bilayer self-assembly. *Structure* **2008**, *16*, 621–630.

(17) Sansom, M. S. P.; Scott, K. A.; Bond, P. J. Coarse grained simulation: a high throughput computational approach to membrane proteins. *Biochem. Soc. Trans.* **2008**, *36*, 27–32.

(18) Wee, C. L.; Bemporad, D.; Sands, Z. A.; Gavaghan, D.; Sansom, M. S. P. SGTx1, a Kv channel gating-modifier toxin, binds to the interfacial region of lipid bilayers. *Biophys. J.* **2007**, *92*, L07–L09.

(19) Wee, C. L.; Balali-Mood, K.; Gavaghan, D.; Sansom, M. S. P. The interaction of phospholipase A2 with a phospholipid bilayer: coarse-grained molecular dynamics simulations. *Biophys. J.* **2008**, *95*, 1649–1657.

(20) Wee, C. L.; Gavaghan, D.; Sansom, M. S. P. Lipid bilayer deformation and the free energy of interaction of a K_v channel gating-modifier toxin. *Biophys. J.* **2008**, *95*, 3816–3826.

(21) Periole, X.; Huber, T.; Marrink, S. J.; Sakmar, T. P. G protein-coupled receptors self-assemble in dynamics simulations of model bilayers. *J. Am. Chem. Soc.* **2007**, *129*, 10126–10132.

(22) Bond, P. J.; Sansom, M. S. P. Bilayer deformation by the Kv channel voltage sensor domain revealed by self-assembly simulations. *Proc. Natl. Acad. Sci. U.S.A.* **2007**, *104*, 2631–2636.

(23) Venturoli, M.; Smit, B.; Sperotto, M. M. Simulation studies of protein-induced bilayer deformations, and lipid-induced protein tilting, on a mesoscopic model for lipid bilayers with embedded proteins. *Biophys. J.* **2005**, *88*, 1778–1798.

(24) Treptow, W.; Marrink, S.-J.; Tarek, M. Gating motions in voltage-gated potassium channels revealed by coarse-grained molecular dynamics simulations. *J. Phys. Chem. B* **2008**, *112*, 3277–3282.

(25) Yefimov, S.; van der Giessen, E.; Onck, P. R.; Marrink, S. J. Mechanosensitive membrane channels in action. *Biophys. J.* **2008**, *94*, 2994–3002.

(26) Hall, B. A.; Sansom, M. S. P. Coarse-grained MD simulations and protein-protein interactions: the cohesin-dockerin system. *J. Chem. Theory Comput.* **2009**, *5*, 2465–2471.

(27) Lindahl, E.; Sansom, M. S. P. Membrane proteins: molecular dynamics simulations. *Curr. Opin. Struct. Biol.* **2008**, *18*, 425–431.

(28) Bond, P. J.; Wee, C. L.; Sansom, M. S. P. Coarse-grained molecular dynamics simulations of the energetics of helix insertion into a lipid bilayer. *Biochemistry* **2008**, *47*, 11321–11331.

(29) Monticelli, L.; Kandasamy, S. K.; Periole, X.; Larson, R. G.; Tieleman, D. P.; Marrink, S. J. The MARTINI coarse grained force field: extension to proteins. *J. Chem. Theory Comput.* **2008**, *4*, 819–834.

(30) Psachoulia, E.; Bond, P. J.; Fowler, P. W.; Sansom, M. S. P. Helix-helix interactions in membrane proteins: coarse grained simulations of glycophorin helix dimerization. *Biochem.* **2008**, *47*, 10503–105012.

(31) Allen, T. W. Modeling charged protein side chains in lipid membranes. *J. Gen. Physiol.* **2007**, *130*, 237–240.

(32) Vorobyov, I.; Li, L.; Allen, T. W. Assessing atomistic and coarse-grained force fields for protein-lipid interactions: the formidable challenge of an ionizable side chain in a membrane. *J. Phys. Chem. B* **2008**, *112*, 9588–9602.

(33) Chang, R.; Ayton, G. S.; Voth, G. A. Multiscale coupling of mesoscopic- and atomistic-level lipid bilayer simulations. *J. Chem. Phys.* **2005**, *122*, 244716.

(34) Ayton, G. A.; Noid, W. G.; Voth, G. A. Multiscale modeling of biomolecular systems: in serial and in parallel. *Curr. Opin. Struct. Biol.* **2007**, *17*, 192–198.

(35) Ayton, G. S.; Voth, G. A. Multiscale simulation of transmembrane proteins. *J. Struct. Biol.* **2007**, *157*, 570–578.

(36) Ayton, G. S.; Voth, G. A. Systematic multiscale simulation of membranes protein systems. *Curr. Opin. Struct. Biol.* **2009**, *19*, 138–144.

(37) Carpenter, T.; Bond, P. J.; Khalid, S.; Sansom, M. S. P. Self-assembly of a simple membrane protein: coarse-grained molecular dynamics simulations of the influenza M2 channel. *Biophys. J.* **2008**, *95*, 3790–3801.

(38) Orsi, M.; Sanderson, W. E.; Essex, J. W. Permeability of small molecules through a lipid bilayer: a multiscale simulation study. *J. Phys. Chem. B* **2009**, *113*, 12019–12029.

(39) Ruta, V.; Jiang, Y. X.; Lee, A.; Chen, J. Y.; MacKinnon, R. Functional analysis of an archaebacterial voltage-dependent K^+ channel. *Nature* **2003**, *422*, 180–185.

(40) Jiang, Y.; Ruta, V.; Chen, J.; Lee, A. G.; Mackinnon, R. The principle of gating charge movement in a voltage-dependent K^+ channel. *Nature* **2003**, *423*, 42–48.

(41) Swartz, K. J. Tarantula toxins interacting with voltage sensors in potassium channels. *Toxicon* **2007**, *49*, 213–230.

(42) Milescu, M.; Vobecky, J.; Roh, S. H.; Kim, S. H.; Jung, H. J.; Il Kim, J.; Swartz, K. J. Tarantula toxins interact with voltage sensors within lipid membranes. *J. Gen. Physiol.* **2007**, *130*, 497–511.

(43) Takahashi, H.; Kim, J. I.; Min, H. J.; Sato, K.; Swartz, K. J.; Shimada, I. Solution structure of hanatoxin1, a gating modifier of voltage- dependent K^+ channels: Common surface features of gating modifier toxins. *J. Mol. Biol.* **2000**, *297*, 771–780.

(44) Jung, H. J.; Lee, J. Y.; Kim, S. H.; Eu, Y. J.; Shin, S. Y.; Milescu, M.; Swartz, K. J.; Kim, J. I. Solution structure and lipid membrane partitioning of VSTx1, an inhibitor of the KvAP potassium channel. *Biochemistry* **2005**, *44*, 6015–6023.

(45) Lee, C. W.; Kim, S.; Roh, S. H.; Endoh, H.; Kodera, Y.; Maeda, T.; Kohno, T.; Wang, J. M.; Swartz, K. J.; Kim, J. I. Solution structure and functional characterisation of SGTx1, a modifier of Kv2.1 channel gating. *Biochemistry* **2004**, *43*, 890–897.

(46) Jung, H. J.; Lee, J. Y.; Kim, S. H.; Eu, Y. J.; Shin, S. Y.; Milescu, M.; Swartz, K. J.; Kim, J. I. Solution structure and lipid membrane partitioning of VSTx1, an inhibitor of the KvAP potassium channel. *Biochemistry* **2005**, *44*, 6015–6023.

(47) Phillips, L. R.; Milescu, M.; Li-Smerin, Y.; Midell, J. A.; Kim, J. I.; Swartz, K. J. Voltage-sensor activation with a tarantula-toxin as cargo. *Nature* **2005**, *436*, 857–860.

(48) Lee, S. Y.; MacKinnon, R. A membrane-access mechanism of ion channel inhibition by voltage sensor toxins from spider venom. *Nature* **2004**, *430*, 232–235.

(49) Bemporad, D.; Wee, C. L.; Sands, Z.; Grottesi, A.; Sansom, M. S. P. VSTx1, a modifier of Kv channel gating, localizes to the interfacial region of lipid bilayers. *Biochemistry* **2006**, *45*, 11844–11855.

(50) Ulmschneider, M. B.; Sansom, M. S. P.; Di Nola, A. Properties of integral membrane protein structures: derivation of an implicit membrane potential. *Proteins: Struct., Funct., Bioinf.* **2005**, *59*, 252–265.

(51) Dominy, B. N.; Brooks, C. L. Development of a generalized Born model parameterisation for proteins and nucleic acids. *J. Phys. Chem. B* **1999**, *103*, 3765–3773.

(52) Lee, M. S.; Salsbury, F. R.; Brooks, C. L. Novel generalized Born methods. *J. Chem. Phys.* **2002**, *116*, 10606–10614.

(53) Roux, B. The calculation of the potential of mean force using computer simulations. *Comput. Phys. Commun.* **1995**, *91*, 275–282.

(54) Torrie, G. M.; Valleau, J. P. Nonphysical sampling distributions in Monte-Carlo free energy distributions: umbrella sampling. *J Comput. Phys.* **1977**, *23*, 187–199.

(55) Kumar, S.; Bouzida, D.; Swendsen, R. H.; Kollman, P. A.; Rosenberg, J. M. The weighted histogram analysis method for free-energy calculations on biomolecules. 1. The method. *J. Comput. Chem.* **1992**, *13*, 1011–1021.

(56) Wang, J. M.; Roh, S. H.; Kim, S.; Lee, C. W.; Kim, J. I.; Swartz, K. J. Molecular surface of tarantula toxins interacting with voltage sensors in Kv channels. *J. Gen. Physiol.* **2004**, *123*, 455–467.

(57) Eisenberg, D.; Schwarz, E.; Komaromy, M.; Wall, R. Analysis of membrane and surface protein sequences with the hydrophobic moment plot. *J. Mol. Biol.* **1984**, *179*, 125–142.

(58) Krznaric, D.; Levcopoulos, C. Fast algorithms for complete linkage clustering. *Discrete Comp. Geom.* **1998**, *19*, 131–145.

(59) Bond, P. J.; Sansom, M. S. P. Insertion and assembly of membrane proteins via simulation. *J. Am. Chem. Soc.* **2006**, *128*, 2697–2704.

(60) Lindahl, E.; Hess, B.; van der Spoel, D. GROMACS 3.0: a package for molecular simulation and trajectory analysis. *J. Mol. Model.* **2001**, *7*, 306–317.

(61) van der Spoel, D.; Lindahl, E.; Hess, B.; Groenhof, G.; Mark, A. E.; Berendsen, H. J. GROMACS: fast, flexible, and free. *J. Comput. Chem.* **2005**, *26*, 1701–1718.

(62) van Gunsteren, W. F.; Kruger, P.; Billeter, S. R.; Mark, A. E.; Eising, A. A.; Scott, W. R. P.; Huneberger, P. H.; Tironi, I. G. *Biomolecular Simulation: The GROMOS96 Manual and User Guide*; Biomos & Hochschulverlag AG an der ETH Zurich: Groningen; Zurich, 1996.

(63) Berger, O.; Edholm, O.; Jahnig, F. Molecular dynamics simulations of a fluid bilayer of dipalmitoylphosphatidycholine at full hydration, constant pressure and constant temperature. *Biophys. J.* **1997**, *72*, 2002–2013.

(64) Marrink, S. J.; Berger, O.; Tieleman, D. P.; Jahnig, F. Adhesion forces of lipids in a phospholipid membrane studied by molecular dynamics simulations. *Biophys. J.* **1998**, *74*, 931–943.

(65) Hermans, J.; Berendsen, H. J. C.; van Gunsteren, W. F.; Postma, J. P. M. A consistent empirical potential for water-protein interactions. *Biopolymers* **1984**, *23*, 1513–1518.

(66) Darden, T.; York, D.; Pedersen, L. Particle mesh Ewald - an N.log(N) method for Ewald sums in large systems. *J. Chem. Phys.* **1993**, *98*, 10089–10092.

(67) Hess, B.; Bekker, H.; Berendsen, H. J. C.; Fraaije, J. G. E. M. LINCS: A linear constraint solver for molecular simulations. *J. Comput. Chem.* **1997**, *18*, 1463–1472.

(68) Miyamoto, S.; Kollman, P. A. Settle - an analytical version of the Shake and Rattle algorithm for rigid water models. *J. Comput. Chem.* **1992**, *13*, 952–962.

(69) Berendsen, H. J. C.; Postma, J. P. M.; van Gunsteren, W. F.; DiNola, A.; Haak, J. R. Molecular dynamics with coupling to an external bath. *J. Chem. Phys.* **1984**, *81*, 3684–3690.

(70) Ulmschneider, J. P.; Ulmschneider, M. B. Folding simulations of the transmembrane helix of Virus Protein U in an implicit membrane model. *J. Chem. Theory Comput.* **2007**, *3*, 2335–2346.

(71) Qiu, D.; Shenkin, P. S.; Hollinger, F. P.; Still, C. W. The GB/SA continuum model for solvation. A fast analytical method for the calculation of approximate Born radii. *J. Phys. Chem. A* **1997**, *101*, 3005–3014.

(72) Jorgensen, W. L.; Ulmschneider, J. P.; Tirado-Rives, J. Free energies of hydration from a generalized Born model and an ALL-atom force field. *J. Phys. Chem. B* **2004**, *108*, 16264–16270.

(73) Parsegian, A. Energy of an ion crossing a low dielectric membrane: Solution to four relevant electrostatics problems. *Nature* **1969**, *221*, 844–846.

(74) Spassov, V. Z.; Yan, L.; Szalma, S. Introducing an implicit membrane in generalized Born/solvent accessibility continuum solvent models. *J. Phys. Chem. B* **2002**, *106*, 8726–2738.

(75) Killian, J. A. Synthetic peptides as models for intrinsic membrane proteins. *FEBS Lett.* **2003**, *555*, 134–138.

(76) de Planque, M. R. R.; Killian, J. A. Protein-lipid interactions studied with designed transmembrane peptides: role of hydrophobic matching and interfacial anchoring. *Mol. Membr. Biol.* **2003**, *20*, 271–284.

(77) Wiener, M. C.; White, S. H. Structure of a fluid dioleoylphosphatidylcholine bilayer determined by joint refinement of X-ray and neutron diffraction data. III. Complete structure. *Biophys. J.* **1992**, *61*, 434–447.

(78) Kaminski, G. A.; Friesner, R. A.; Tirado-Rives, J.; Jorgensen, W. L. Evaluation and reparametrization of the OPLS-AA force field for proteins via comparison with accurate quantum chemical calculations on peptides. *J. Phys. Chem. B* **2001**, *105*, 6474–6487.

(79) Radzicka, A.; Wolfenden, R. Comparing the polarities of the amino acids: side-chain distribution coefficients between the vapor phase, cyclohexane, 1-octanol, and neutral aqueous solution. *Biochemistry* **1988**, *27*, 1664–1670.

(80) Nishizawa, M.; Nishizawa, K. Interaction between K^+ channel gate modifier hanatoxin and lipid bilayer membranes analyzed by molecular dynamics simulation. *Eur. Biophys. J.* **2006**, *35*, 373–381.

(81) Alabi, A. A.; Bahamonde, M. I.; Jung, H. J.; Kim, H. J.; Swartz, K. J. Portability of paddle motif function and pharmacology in voltage sensors. *Nature* **2007**, *450*, 370–375.

(82) Schmidt, D.; MacKinnon, R. Voltage-dependent K^+ channel gating and voltage sensor toxin sensitivity depend on the mechanical state of the lipid membrane. *Proc. Natl. Acad. Sci. U.S.A.* **2008**, *105*, 19276–19281.

(83) Swartz, K. J. Sensing voltage across lipid membranes. *Nature* **2008**, *456*, 891–897.

(84) Posokhov, Y. O.; Gottlieb, P. A.; Morales, M. J.; Sachs, F.; Ladokhin, A. S. Is lipid bilayer binding a common property of inhibitor cysteine knot ion-channel blockers? *Biophys. J.* **2007**, *93*, L20–L22.

(85) Wee, C. L.; Sansom, M. S. P.; Reich, S.; Akhmatskaya, E. Improved sampling for simulations of interfacial membrane proteins: application of Generalized Shadowing Hybrid Monte Carlo to a peptide toxin/bilayer system. *J. Phys. Chem. B* **2008**, *112*, 5710–5717.

(86) Sugita, Y.; Okamoto, Y. Replica-exchange molecular dynamics method for protein folding. *Chem. Phys. Lett.* **1999**, *314*, 141–151.

CT900652S